

Effect of Couette Type of Shear Stress Field with Axial Shear Slope on Deformation and Migration of Cell: Comparison between C2C12 and HUVEC

Shigehiro HASHIMOTO, Hiromi SUGIMOTO, Haruka HINO

Biomedical Engineering, Department of Mechanical Engineering,
Kogakuin University, Tokyo, 163-8677, Japan
shashimoto@cc.kogakuin.ac.jp <http://www.mech.kogakuin.ac.jp/labs/bio/>

ABSTRACT

A shear flow device contained in the microscope incubator has newly been designed to study the effect of the shear stress field on the biological cell *in vitro*. The culture medium was sandwiched with a constant gap between a lower stationary culture plate and an upper rotating parallel plate to make a Couette type of shear field with the perpendicular shear slope. The wall shear stress (τ) on the lower culture disk was controlled by the rotating speed of the upper disk. The shear stress τ increases in proportion to the distance from the axis of rotation. After cultivation for 24 hours for adhesion of cells on the lower plate without flow, $\tau < 2$ Pa was applied on cells for 24 hours subsequently. HUVEC (human umbilical vein endothelial cell) tends to be elongated and aligned under < 2 Pa of the shear stress. C2C12 (mouse myoblast cell line), on the other hand, maintains elongated shape and tends to migrate to the lower shear stress direction (< 2 Pa). The experimental system is useful to study the quantitative relationships between the shear stress and the cell behaviors: deformation, orientation, and migration.

Keywords: Biomedical Engineering, Shear Stress, C2C12, HUVEC and Couette Flow.

1. INTRODUCTION

The cell culture technique has been developed and behavior of biological cells has been observed by several kinds of devices *in vitro*. After adhesion to the scaffold, the cell shows a variety of behaviors: deformation, orientation, and migration. These behaviors depend on several stimulations: electric [1], magnetic [2], and mechanical [3]. The mechanical stimulation is focused in the present study. The cells are exposed to mechanical stimulation *in vivo*. Cells, for instance, are exposed to tensile force field around the skeletal tissue. Myotubes make orientation along the muscle tissue. Endothelial cells, on the other hand, are exposed to the shear stress in the blood flow. The endothelial cells make orientation on the inner surface of the vessel wall.

Several devices have been designed to observe the cells response to the mechanical stress field. In these devices, the special notice should be paid to the transmission point of the mechanical stress to the specimen. In many studies, the stress is applied to the scaffold [3, 4] to evaluate the effects of the stress on alignment [3] and on differentiation [4] of cells. When the slip between the cell and the scaffold occurs, the stress is not transmitted to the cell. A field, on the other hand, is effective to transmit stimulation to the cell placed in the

field: the vibrating field [5] the gravitational field [6], or the flow field [7]. A cell exposed to the flow directly receives the shear stress in the shear flow field regardless of the position of the cell in the fluid.

In the previous study with the vortex flow by the swinging plate *in vitro*, C2C12 (mouse myoblast cell line) made orientation perpendicular to the direction of the flow, although HUVEC (human umbilical vein endothelial cell) made orientation along the streamline of the flow [8]. The orientation of each cell in the tissue depends on that of neighbor's cell. To analyze the mechanism of making orientation of a cell, the behavior of the single cell in the shear flow field should be quantitatively observed *in vitro*. A shear stress lower than 2 Pa is typical at the wall of the blood vessel *in vivo*. At the wall shear stress higher than 2 Pa, a cell showed the following responses in the previous studies: exfoliation from the wall of the scaffold, deformation to be rounded, elongation, and tilt to the streamline [9]. In the Poiseuille type of flow, the shear rate depends on the distance from the wall: highest at the wall. In the Couette type of flow, on the other hand, the shear rate is constant regardless of the distance from the wall. To control the value of the shear stress, the Couette type of flow is stable compared with the Poiseuille type of flow.

In the present study, an experimental system of the Couette type flow in the constant gap with a rotating disk has been designed to apply the shear stress field with the perpendicular shear slope on the cell during incubation at the microscopic observation *in vitro*, and the effect of the shear stress field (< 2 Pa) on the cell has been studied about deformation, orientation, and migration. The range of the shear stress is set lower than 2 Pa, which is typical value at the blood vessel wall.

2. METHODS

Couette Type of Shear Flow Device

A Couette type of shear flow device has been designed in the present study: between a rotating disk and a stationary dish (Fig. 1). The medium is sheared between a rotating wall and a stationary wall. The stationary wall is the bottom of the culture dish (diameter 60 mm) (Fig. 2). In the device, the shear rate (γ) in the medium is calculated by Eq. 1.

$$\gamma = r \omega / d \quad (1)$$

In Eq. 1, ω is the angular velocity [rad s^{-1}], and d is the distance [m] between the wall of the moving disk and the wall of stationary plate. Between the parallel walls, d is constant (Fig. 1). The shear rate (γ [s^{-1}]) in the gap between walls

increases in proportion to the distance (r [m]) from the rotating axis.

The angular velocity ω was controlled by the stepping motor between 5.2 rad s^{-1} and 36 rad s^{-1} . In the observation area of the microscope, r varies between 12 mm and 18 mm. The distance d is 0.5 mm, which is estimated by the positions of the focus of the walls at the microscope. These parameters make variations on the shear rates ($\dot{\gamma}$) between $0.12 \times 10^3 \text{ s}^{-1}$ and $1.3 \times 10^3 \text{ s}^{-1}$. The shear stress (τ [Pa]) is calculated by the viscosity (η [Pa s]) of the medium.

$$\tau = \eta \dot{\gamma} \quad (2)$$

Using the viscosity of the medium of $1.5 \times 10^{-3} \text{ Pa s}$ (measured at 310 K by a cone and plate viscometer), the variations of the shear stress τ have been calculated as the value between 0.18 Pa and 2.0 Pa. The rotating disk device is mounted on the stage of the inverted phase contrast microscope placed in the incubator (Fig. 2). The device allows the microscopic observation of cells cultured on the stationary wall during exposure to the shear flow.

Measurement of Cell

The time-lapse microscopic images were taken every five minutes during the cultivation. The contour of each cell adhered on the stationary plate of the scaffold was traced (Fig. 3), and the projected two-dimensional area (S) at the image of each cell was calculated. The expansion rate of the area per hour (R_s [hour $^{-1}$]) was calculated by tracing the same cell at the time lapse image.

$$R_s = (S_2 - S_1) / S_1 \quad (3)$$

In Eq. 3, the area S_2 is measured after one hour at the traced cell, which had the area of S_1 . When the area increases, the rate (R_s) becomes positive. Unity of R_s means that the area is doubled. When the area decreases faster, the value of R_s approaches to minus unity. The contour of each cell was approximated to an ellipsoid, and the shape index (Z) was calculated by Eq. 4.

$$Z = 1 - (b / a) \quad (4)$$

In Eq. 4, a is the lengths of the major axis, and b is the length of the minor axis (Fig. 3). The shape index (Z) equals to zero at the circle ($a = b$). The shape index approaches to unity, as the cell elongates ($a \gg b$). The elongation rate of the shape index per hour (R_z [hour $^{-1}$]) was calculated by tracing the same cell at the time lapse image.

$$R_z = (Z_2 - Z_1) / Z_1 \quad (5)$$

In Eq. 5, the shape index Z_2 is measured after one hour at the traced cell, which had the shape index of Z_1 . When the shape index increases, the rate (R_z) becomes positive. Unity of R_z means that the shape index is doubled. When the shape index decreases faster, the value of R_s approaches to minus unity. The actual direction of the steady flow adjacent to the scaffold surface of the culture plate was traced by the moving particle adjacent to the surface at the microscopic video image, and defined as the x axis direction in Figs. 14–17. The direction was also confirmed by the movement of the micro spheres rolling on the surface at the extra flow test. The acute angle (0 degree $< \theta < 90$ degree) between the major axis and x axis was

measured at the microscopic image of each cell. The centroid of each ellipsoid was used to trace the migration of the cell at the microscopic time lapse images. The direction of y axis is defined perpendicular to the x axis. The distance of migration per hour (D) was measured at each component: D_x , and D_y . The positive value of D_x coincides with downstream migration. The positive value of D_y coincides with migration to the center of the rotation.

3. RESULTS

In Figs. 4–10, each datum point at 0 Pa shows control datum without exposure to the shear field. In Figs. 4–10, data belong to the same test are categorized by the same character of the marker. As each cell migrates, r varies. Each shear stress is calculated using each r at the present centroid of the cell (Fig. 3). In each test, the shear stress applied on each cell can vary in the range of mean $\pm 20\%$ with the variation of r even at the fixed observation area of the microscope.

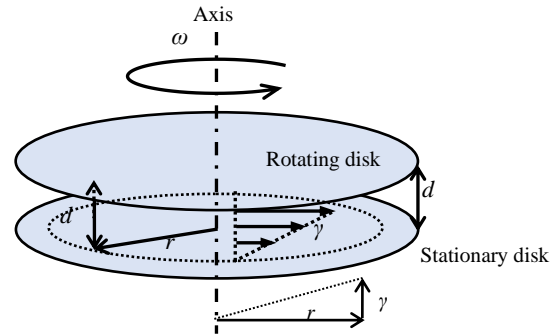


Fig. 1: Couette flow between rotating disk and stationary disk: shear rate ($\dot{\gamma}$) increases with distance from axis (r).

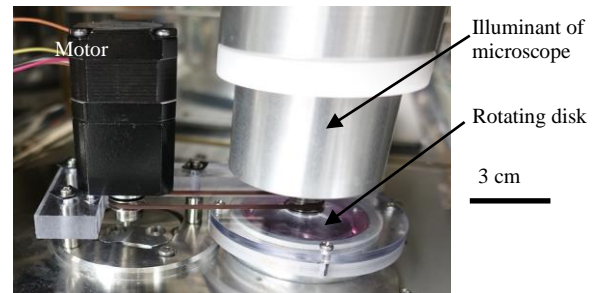


Fig. 2: Couette flow device in incubator.

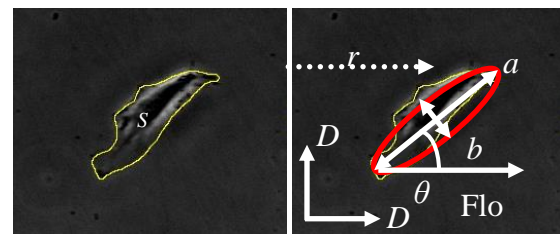


Fig. 3: Cell contour is traced (left), and approximated to ellipsoid (right).

Fig. 4 shows the area S of each cell related to the shear stress after exposure to the shear field for 24 hours. In Fig. 4A, several cells of C2C12 expand to have the area larger than 0.005 mm^2 at the shear stress (τ) higher than 0.3 Pa . At the shear stress of 0.8 Pa , some cells of C2C12 expand to have the area larger than 0.02 mm^2 . The area of each cell of C2C12 is most changeable at the shear stress of 0.8 Pa . In Fig. 4B, some cells of HUVEC expand their own area even without the flow stimulation (at 0 Pa). The area of HUVEC is relatively small at the shear stress higher than 1.5 Pa . The highest expansion of the area of HUVEC occurs at the shear stress around 1 Pa .

Fig. 5 shows the expansion rate of the area of each cell per hour (R_s). In Fig. 5A, the area of each cell of C2C12 changes every hour, even under no flow condition (0 Pa). The expansion rate is high around the shear stress of 1.5 Pa . The expansion rate becomes significantly low at 2 Pa . The data of the expansion rate of HUVEC concentrate in slightly lower range than that of C2C12. A few cells show the high rate (R_s) at the shear stress between 0.5 Pa and 1.5 Pa (Fig. 5B).

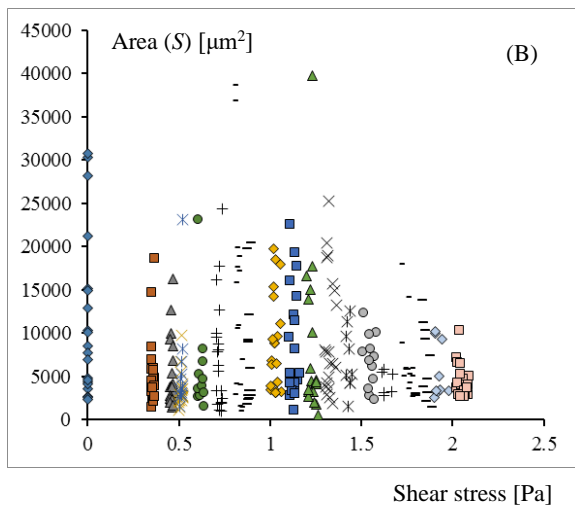
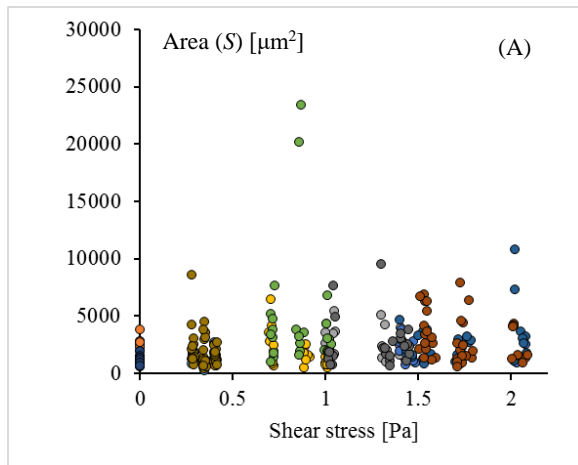


Fig. 4: After shear stimulation for 24 hour, area S of C2C12 (A), and of HUVEC (B).

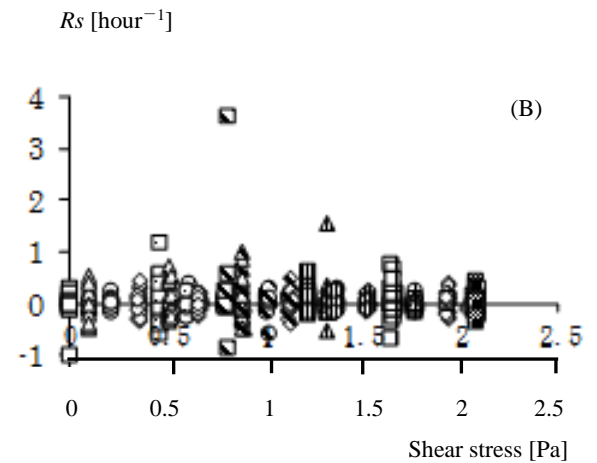
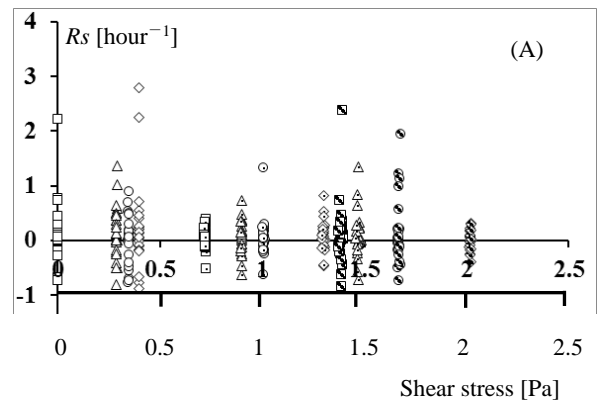


Fig. 5: Expansion rate of area per hour (R_s) of C2C12 (A), and of HUVEC (B).

Fig. 6 shows the shape index (Z) of each cell, after the flow stimulation for 24 hours. Without the flow stimulation (0 Pa), the shape index distributes over the wide range of Z at random, which corresponds to the random deformation of each cell. Some cells of C2C12 elongate at 0 Pa . Some cells elongate at the shear stress $< 1 \text{ Pa}$. The ratio of elongated cells (shape index > 0.5) decreases at the shear stress $> 1.5 \text{ Pa}$. The number of rounded cells (shape index < 0.5) decreases because of exfoliation after exposure to the shear field. Many cells elongate at the shear stress around 1 Pa . Many cells are exfoliated at 2 Pa .

Fig. 7 shows the elongation rate of the shape index of each cell per hour (R_z). The rate of C2C12 is sometimes higher at the shear stress around 0.3 Pa . The elongation rate becomes significantly lower at the shear stress higher than 1.5 Pa . The rate of HUVEC is significantly lower than that of C2C12 at the shear stress lower than 0.5 Pa .

Fig. 8 shows the angle (θ) between the major axis of the cell and the flow direction after flow stimulation for 24 hours. Zero degree corresponds to the flow direction. Data of the angle distribute in the whole range at random at 0 Pa (without flow). The number of cells of C2C12 decreases at the larger angle at 2 Pa (Fig. 8A). Several cells of C2C12 tilt to the angle larger

than 45 degree from the flow direction at the shear stress lower than 2 Pa (Fig. 8A). The number of HUVEC at the angle around 0 degree increases at the shear stress around 1 Pa (Fig. 8B). The number of HUVEC decreases at the angle between the longitudinal axis and the flow direction around 45 degree, especially at the higher wall shear stress.

Fig. 9 shows x component (flow direction) migration Dx of each cell per hour. Each cell migrates at random (-0.05 mm/hour $< Dx < 0.05$ mm/hour) at 0 Pa (without flow). C2C12 tends to migrate to the downstream direction (positive value at Fig. 14) at 2 Pa. In Fig. 9B, the migration of HUVEC at the direction parallel to the flow increases at the shear stress around 0.7 Pa. The migration to the upstream direction (negative Dx), on the other hand, decreases at the wall shear stress higher than 1.5 Pa.

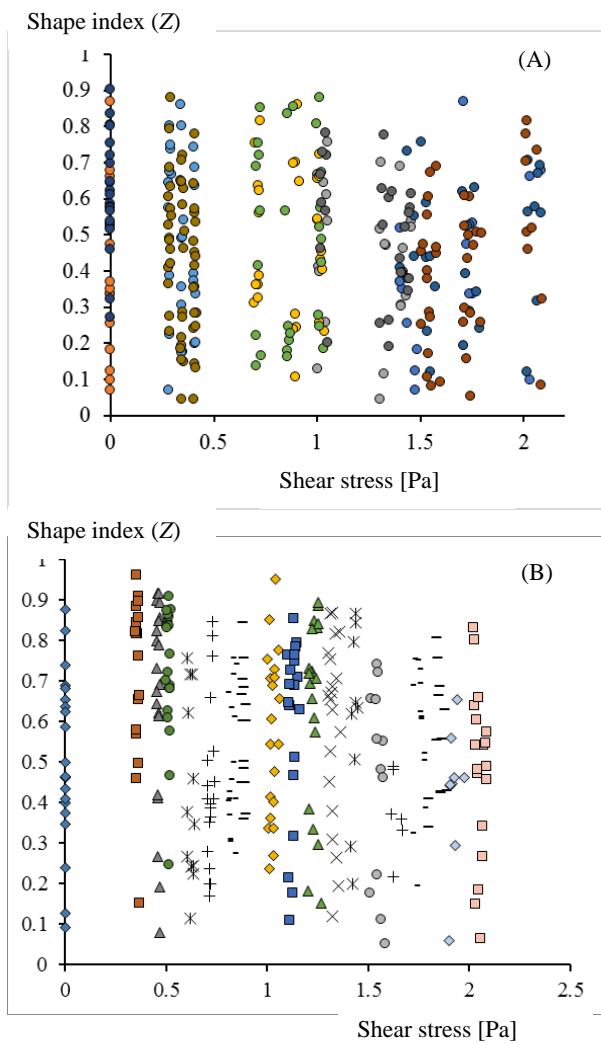


Fig. 6: After flow stimulation for 24 hours, shape index (Z) of C2C12 (A), and of HUVEC (B).

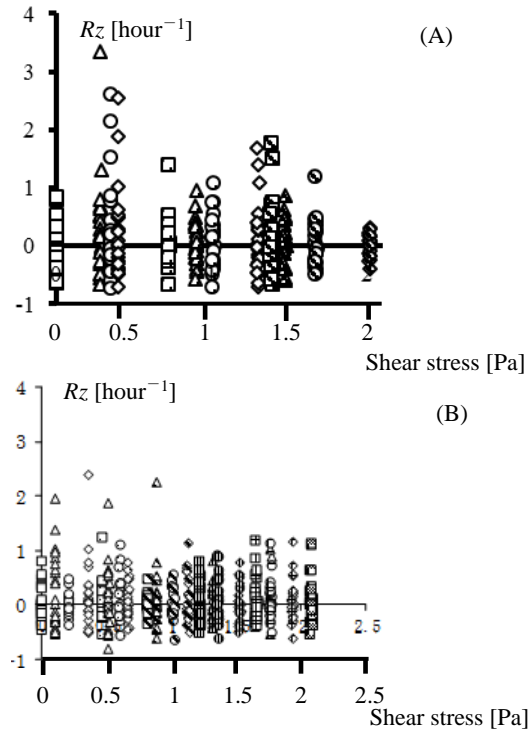


Fig. 7: Elongation rate (Rz) of shape index (Z): C2C12 (A), and HUVEC (B).

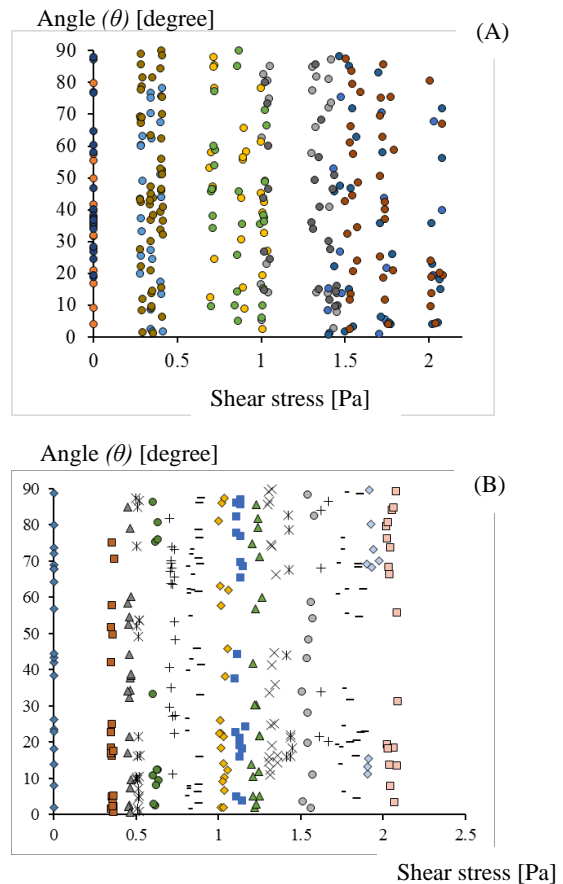


Fig. 8: After flow stimulation 24 hours, angle (θ) of C2C12 (A), and of HUVEC (B).

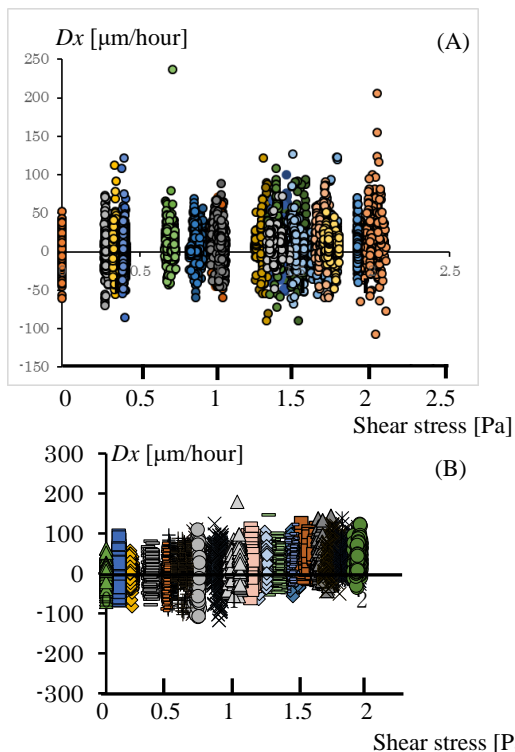


Fig. 9: Migration D_x (flow direction) per hour of C2C12 (A), HUVEC (B).

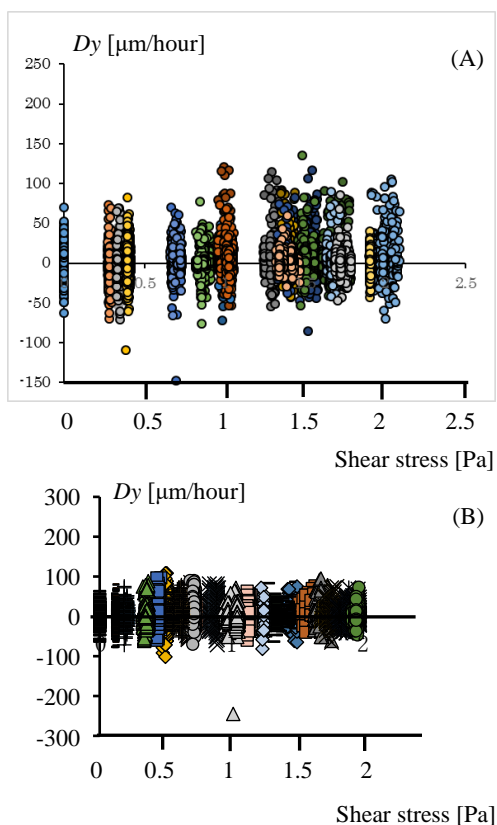


Fig. 10: Migration D_y (perpendicular to the flow direction) per hour of C2C12 (A), HUVEC (B).

Fig. 10 shows y component (perpendicular to the flow direction) migration D_y of each cell per hour. Each cell migrates at random ($-0.05 \text{ mm}/\text{hour} < D_y < 0.05 \text{ mm}/\text{hour}$) at 0 Pa (without flow). Around 1 Pa, C2C12 tends to migrate to the area of the lower shear stress. The positive data shift in Fig. 10B corresponds to the approach to the rotating axis. Absolute value of migration of HUVEC to the perpendicular direction to the flow shows the peak value at the shear stress around 0.5 Pa. Different from C2C12, the distribution of the migration of HUVEC does not show the bias at D_y .

4. DISCUSSION

In the previous study, cells were exposed to the shear flow in a donut-shaped open channel, and the effect of flow stimulation on cultured cells has been studied *in vitro* [8]. When the flow has a free surface, it is difficult to estimate the shear stress value in the fluid. Between two parallel walls, on the other hand, the velocity profile is estimated in the laminar flow. In the previous studies, several preparations were designed to study the effect of mechanical stimulations on biological cells: tilting disk [9], rhombus [10], cross [11], and rotating disks types [12]. The Couette type of flow is selected in the present study for the quantitative evaluation of the effect of the shear stress on cells.

The Couette type of flow is convenient to estimate the shear stress in the flow with the uniform shear rate between the moving wall and the stationary wall, which is also available to non-Newtonian fluid. Several kinds of the devices of Couette type flow were designed for quantitative experiments of biological fluid in the previous studies.

The “cone and plate type” device has the uniform shear field in the entire space between the rotating cone and the stationary plate. The shear stress is constant independent of the distance from the rotating axis. The clot formation was quantitatively studied between the rotating cone and the stationary plate [13], and between the rotating concave cone and the stationary convex cone [14]. The erythrocyte destruction was studied between the rotating concave cone and the stationary convex cone [15]. A parallel disks system between rotating disk and the stationary disk, on the other hand, has several advantages: stability of the rotating motion of the disk, stability of the optical path for the microscopic observation, morphologic preciseness of the plane of the disks, and simultaneous observation over the range of variation of shear rate proportional to the radius from the rotational axis. The counter rotating parallel discs system was used for observation of deformation [16], and the sublethal damage [17] of the erythrocyte. In the present study, the rotating parallel disk system is selected to make Couette type of flow instead of the cone and plate system. At the constant angular velocity of 36 rad s^{-1} ($d = 0.5 \text{ mm}$), the shear rate ($\dot{\gamma}$) increases from $0.87 \times 10^3 \text{ s}^{-1}$ to $1.3 \times 10^3 \text{ s}^{-1}$, when the distance from the axis (r) increases from 12 mm to 18 mm in the observation area (Eq. 1). The range of the shear rate enables the simultaneous observation of the behavior of cells related to variation of the shear stress (between 1.3 Pa and 2.0 Pa) in the same view [12]. The observed migration speed was slower than $10 \text{ nm}/\text{s}$ in the test. The rotating flow might induce the secondary flow by the centrifugal effect. The rotational speed of the disk is smaller than 0.7 m s^{-1} in the present system. The microscopic video

image of the flowing cells between the rotating disk and the stationary disk shows the steady flow. Reynolds number (Re) is calculated by Eq. 6.

$$Re = \rho v d / \eta = \rho r \omega d / \eta \quad (6)$$

In Eq. 6, ρ is density of the fluid [kg m^{-3}], v is the circumferential velocity [m s^{-1}], ω is the angular velocity [rad s^{-1}], r is the distance [m] from the rotating axis, d is the distance [m] between the moving wall and the stationary wall, and η is the viscosity of the fluid [Pa s]. Re is 2.2×10^2 , when ρ , r , ω , d , and η are $1 \times 10^3 \text{ kg m}^{-3}$, 0.018 m , 36 rad s^{-1} , 0.0005 m , and 0.0015 Pa s , respectively. The turbulent flow may not occur in the flow of the small value of Reynolds number. The steady actual flow direction adjacent to the scaffold surface of cell culture has been confirmed by the streamline traced by the direction of exfoliation of the cell and of the moving particle adjacent to the surface.

Endothelial cells are exposed to the shear flow in the blood vessels *in vivo*. The effect of shear flow on endothelial cells was investigated in the previous studies [18]. Cells are not exfoliated under the shear flow at the wall shear stress lower than 1.5 Pa. Cells were exfoliated at the higher wall shear stress in the previous studies [9]. A biological cell shows passive and active responses in an environment [19]. While the flow enhances the cell migration to the downstream direction, a cell migrates to adapt to the shear field. While the strong stimulation above the threshold damages the cell, the stimulation below the threshold remains in the cell as a memory for the response in the next step [20]. The hysteresis effect governs the active response of the cell [21].

The interaction between cells also governs the behavior of each cell. The orientation of each cell depends also on the orientation of the neighbor cell. The low seeding density is chosen in this study to track images of each cell. The migration of the cell might also depend on the morphology [22] and the mechanical property of the scaffold [23, 24].

In the present study, each cell migrates to every direction includes the counter direction of the flow. The most of myoblasts tend to migrate to the oblique direction of the lower shear stress field at 1 Pa. The effect of shear flow on migration of the cell depends on the cell types. The dependency might be applied to the cell sorting technology. The quantitative relationships between the shear stress and the cell orientation might be applied to tissue technology to control of cells *in vitro*.

In the previous study, C2C12 made orientation perpendicular to the direction of the flow, although HUVEC made orientation along the streamline of the flow [8]. In the present study at the shear stress around 1.5 Pa, C2C12 tends to migrate to the perpendicular lower shear stress direction. The tendency cannot be observed in the uniform shear field between cone and plate [25]. HUVEC, on the other hand, tends to migrate to the downstream direction in the present study at the shear stress around 1.5 Pa. HUVEC tends to make orientation along the flow direction at the shear stress around 1 Pa. The perpendicular shear slope (τ / r) cannot be controlled independent of τ in the present device (Eq. 7).

$$\tau / r = \eta \omega / d \quad (7)$$

5. CONCLUSION

In the present study, a Couette type of a shear flow device with parallel walls placed at the microscope in the incubator has been designed to measure the orientation and the migration of the cultured biological cell in the shear stress field *in vitro*. The time-laps images show that every cell keeps movement under the shear flow: migration and deformation (elongation and contraction). The movement decreases under the high shear stress ($> 1.5 \text{ Pa}$). Some cells show responses dependent to the shear flow: orientation to the flow direction, migration to the downstream direction, deformation to the rounded shape, and exfoliation. At the shear stress around 1.0 Pa, on the other hand, each cell deforms and migrates to any direction independent of the flow direction. The deformation of C2C12 is more frequent than that of HUVEC. At the shear stress around 1.5 Pa, some cells of C2C12 migrate to the lower shear stress area. The quantified mechanism would be applied to the engineered tissue fabrication. The manufactured experimental system of Couette type of the shear field with the perpendicular shear slope is effective to measure the response (deformation, orientation, and migration) of cells to the shear stress quantitatively.

6. ACKNOWLEDGMENT

This work was supported by a Grant-in-Aid for Strategic Research Foundation at Private Universities from the Japanese Ministry of Education, Culture, Sports and Technology. The authors thank to Prof. Richard Magin for discussion of the contents of the article.

REFERENCES

- [1] S. Hashimoto, F. Sato, R. Uemura and A. Nakajima, "Effect of Pulsatile Electric Field on Cultured Muscle Cells In Vitro", **Journal of Systemics Cybernetics and Informatics**, Vol. 10, No. 1, 2012, pp. 1–6.
- [2] S. Hashimoto and K. Tachibana, "Effect of Magnetic Field on Adhesion of Muscle Cells to Culture Plate", **Journal of Systemics Cybernetics and Informatics**, Vol. 11, No. 4, 2013, pp. 7–12.
- [3] J.H.-C. Wang, E.S. Grood, J. Florer and R. Wenstrup, "Alignment and Proliferation of MC3T3-E1 Osteoblasts in Microgrooved Silicone Substrata Subjected to Cyclic Stretching", **Journal of Biomechanics**, Vol. 33, No. 6, 2000, pp. 729–735.
- [4] G. Yourek, S.M. McCormick, J.J. Mao and G.C. Reilly, "Shear Stress Induces Osteogenic Differentiation of Human Mesenchymal Stem Cells", **Regenerative Medicine**, Vol. 5, No. 5, 2010, pp. 713–724.
- [5] H. Hino, S. Hashimoto, Y. Takahashi and H. Nakajima, "Effect of Ultrasonic Vibration on Proliferation and Differentiation of Cells", **Journal of Systemics, Cybernetics and Informatics**, Vol. 14, No. 6, 2016, pp. 1–7.
- [6] S. Hashimoto, H. Hino and T. Iwagawa, "Effect of Excess Gravitational Force on Cultured Myotubes In Vitro", **Journal of Systemics, Cybernetics and Informatics**, Vol. 11, No. 3, 2013, pp. 50–57.
- [7] M.J. Levesque and R.M. Nerem, "The Elongation and Orientation of Cultured Endothelial Cells in Response to

- Shear Stress”, **Journal of Biomechanical Engineering**, Vol. 107, No. 4, 1985, pp. 341–347.
- [8] S. Hashimoto and M. Okada, “Orientation of Cells Cultured in Vortex Flow with Swinging Plate In Vitro”, **Journal of Systemics Cybernetics and Informatics**, Vol. 9, No. 3, 2011, pp. 1–7.
- [9] S. Hashimoto, F. Sato, H. Hino, H. Fujie, H. Iwata and Y. Sakatani, “Responses of Cells to Flow In Vitro”, **Journal of Systemics Cybernetics and Informatics**, Vol. 11, No. 5, 2013, pp. 20–27.
- [10] F. Sato, S. Hashimoto, T. Yasuda and H. Fujie, “Observation of Biological Cells in Rhombus Parallelepiped Flow Channel”, **Proc. 17th World Multi-Conference on Systemics Cybernetics and Informatics**, Vol. 1, 2013, pp. 25–30.
- [11] H. Hino, S. Hashimoto, Y. Takahashi and S. Nakano, “Design of Cross Type of Flow Channel to Control Orientation of Cell”, **Proc. 20th World Multi-Conference on Systemics Cybernetics and Informatics**, Vol. 2, 2016, pp. 117–122.
- [12] H. Hino, S. Hashimoto, Y. Takahashi and M. Ochiai, “Effect of Shear Stress in Flow on Cultured Cell: Using Rotating Disk at Microscope”, **Journal of Systemics, Cybernetics and Informatics**, Vol. 14, No. 4, 2016, pp. 6–12.
- [13] S. Hashimoto, H. Maeda and T. Sasada, “Effect of Shear Rate on Clot Growth at Foreign Surfaces”, **Artificial Organs**, Vol. 9, No. 4, 1985, pp. 345–350.
- [14] S. Hashimoto, “Clot Growth under Periodically Fluctuating Shear Rate”, **Biorheology**, Vol. 31, No. 5, 1994, pp. 521–532.
- [15] S. Hashimoto, “Erythrocyte Destruction under Periodically Fluctuating Shear Rate; Comparative Study with Constant Shear Rate”, **Artificial Organs**, Vol. 13, No. 5, 1989, pp. 458–463.
- [16] S. Hashimoto, H. Otani, H. Imamura, et al., “Effect of Aging on Deformability of Erythrocytes in Shear Flow”, **Journal of Systemics Cybernetics and Informatics**, Vol. 3, No. 1, 2005, pp. 90–93.
- [17] S. Hashimoto, “Detect of Sublethal Damage with Cyclic Deformation of Erythrocyte in Shear Flow”, **Journal of Systemics Cybernetics and Informatics**, Vol. 12, No. 3, 2014, pp. 41–46.
- [18] M.L.C. Albuquerque, C.M. Waters, U. Savla, H.W. Schnaper and S.A. Flozak, “Shear Stress Enhances Human Endothelial Cell Wound Closure In Vitro”, **American Journal of Physiology - Heart and Circulatory Physiology**, Vol. 279, No. 1, pp. 2000, H293–H302.
- [19] R.H.W. Lam, Y. Sun, W. Chen and J. Fu, “Elastomeric Microposts Integrated into Microfluidics for Flow-mediated Endothelial Mechanotransduction Analysis”, **Lab on Chip**, Vol. 12, No. 10, 2012, pp. 1865–1873.
- [20] W. Yu, H. Qu, G. Hu, Q. Zhang, K. Song, H. Guan, T. Liu and J. Qin, “A Microfluidic-based Multi-shear Device for Investigating the Effects of Low Fluid-induced Stresses on Osteoblasts”, **PLoS ONE**, Vol. 9, No. 2, 2014, pp. 1–7.
- [21] S.D. Tan, T.J. deVries, A.M. Kuijpers-Jagtman, C.M. Semeins, V. Everts and J. Klein-Nulend, “Osteocytes Subjected to Fluid Flow Inhibit Osteoclast Formation and Bone Resorption”, **Bone**, Vol. 41, No. 5, 2007, pp. 745–751.
- [22] H. Hino, S. Hashimoto and F. Sato, “Effect of Micro Ridges on Orientation of Cultured Cell”, **Journal of Systemics Cybernetics and Informatics**, Vol. 12, No. 3, 2014, pp. 47–53.
- [23] C.M. Lo, H.B. Wang, M. Dembo and Y.I. Wang, “Cell Movement is Guided by the Rigidity of the Substrate”, **Biophysical Journal**, Vol. 79, No. 1, 2000, pp. 144–152.
- [24] B.C. Isenberg, P.A. DiMilla, M. Walker, S. Kim and J.Y. Wong, “Vascular Smooth Muscle Cell Durotaxis Depends on Substrate Stiffness Gradient Strength”, **Biophysical Journal**, Vol. 97, No. 5, 2009, pp. 1313–1322.
- [25] S. Hashimoto, H. Sugimoto and H. Hino, “Behavior of Cell in Uniform Shear Flow Field between Rotating Cone and Stationary Plate”, **Journal of Systemics Cybernetics and Informatics**, Vol. 16, No. 2, 2018, pp. 1–7.